TUHH

Hamburg University of Technology

Pavan Vishwanath

Simultaneous localization and mapping for camera-based EEG electrode digitalization

MTEC
Medical Technology | Science | Systems

A project paper written at the Institute of Medical Technology and Intelligent Systems and submitted in partial fulfillment of the requirements for the degree Master of Science.

Author: Pavan Vishwanath

Title: Simultaneous localization and mapping for camera-based EEG electrode digitalization

Date: January 24, 2021

Supervisors: Martin Gromniak (MSc.)
Alexander Schlaefer (Dr.-Ing.)

Referees: Prof. Dr.-Ing. Alexander Schlaefer
Prof. Dr.-Ing. Rolf-Rainer Grigat

1 Introduction

Electroencephalography(EEG) is an electrophysiological monitoring method to record the electrical activity of the brain. EEG measures voltage fluctuations resulting from ionic current within the neurons of the brain with the help of electrodes attached to the scalp [1]. Due to its non-invasive nature, economy, and ease of use, EEG technology is now widely used in clinical medicine to diagnose epilepsy, coma, brain death, etc.[2]. In order to determine the exact source of the brain signal, accurate 3D position of the electodes has to be known. Currently available EEG electrode localization methods are broadly classified as (1) manual methods [3] [4], (2) electromagnetic digitalization [5] [6], (3) ultrasound digitalization [7], (4) magnetic resonance imaging (MRI) assisted methods [8], (5) photogrammetric methods [9] [10] [11] [12]. The recent developments in the areas of high precision time of flight (TOF) depth cameras have led to the possibility of combing High resolution industrial camera and a TOF depth camera for the EEG electrode digitalization. One such system is used in [13] which captures images from five different perspectives (five fixed camera positions) color (RGB) and depth information is fused together to localize the EEG electrodes.

Variety of ododmetry based positioning techniques are available in the field of robotics. The techniques which relies on the 3D point clouds employ scan registration algorithms which finds the best transformation that aligns 2 subsequent point clouds (source and target). Especially in the era of autonomous driving, these algorithms serves as the basis for localizing the car and simultaneously build the map of the environment also to estimate the car's trajectory by fusing the data from variety of sensor suites (sensor fusion). The main scan registration technique is iterative closest point (ICP) algorithm introduced in [14] and many varients have been proposed over the years and selecting the appropriate parameters and configuration differs based on the problem. While using ICP, similar to any odometry systems, inherent accumulation of error at each scan registration leads to the drift in the trajectory estimation. Simultaneous localization and mapping (SLAM) technique is usually the go to solution in order to minimize the drift over time and to obtain the best estimate of the trajectory. SLAM in its probalistic form can be addressed via graph-based formulation by constructing a graph whose nodes represent the robot pose and the edge between 2 nodes act as a noisy odometry constraints and loop closure contraints can be added if the robot revisits the previously visited place. Solution to such a graph based SLAM invloves solving a large error minimization problem [15].

In this thesis work an inexpensive RGBD sensor such as Microsoft Azure Kinect is hand guided around the head with EEG cap in an specific trajectory while performing ICP registration between the scans for camera localization. 3D point clouds required to perform the registration is available as a previous step of the pipeline. A pose-graph is created on the fly whose nodes represent each camera pose along the trajectory. Output of the ICP scan registration is added as a edge connecting 2 subsequent nodes which serves as odmoetry constraints between 2 subsequent camera poses. Each camera pose along with the associated point cloud is added to the map which is being built

simultaneously. Pose-graph is solved each time camera revisits the previously visited places and map will be updated with the corrected poses. The objective of this thesis work is to accuaratly estimate the 3D position of the EEG electrodes by simulataneously localizing the camera and building an EEG electrode map based on scan registration and the pose-graph formulation.

2 Background

2.1 Point cloud registration

The objective of any point cloud registration algorithm is to find the best transformation that aligns 2 point clouds (source and target). The main point cloud registration technique is iterative closest point (ICP) algorithm introduced in [14]. A brief introduction to ICP is provided in this section.

Let $P = \{p_1, p_2, ..., p_m\}$ be the source point cloud set that needs to be aligned with the target point cloud set $Q = \{q_1, q_2, ..., q_n\}$ with correspondenses $C = \{(i, j)\}$.

objective : find the best transformation $T = [R|t]$ that aligns the source point cloud set to the target point cloud set which minimizes the mean square objective function given below.

$$\begin{aligned}
\mathtt{E(R|t)} &= \sum_{(i,j)\in C} \|\boldsymbol{q}_i - \mathtt{R}\boldsymbol{p}_j - \boldsymbol{t}\|^2 \\
&\quad or \\
\mathtt{E(R|t)} &= \sum_{(i,j)\in C} \|\boldsymbol{q}_i - \mathtt{T[R|t]}\boldsymbol{p}_j\|^2
\end{aligned} \tag{2.1}$$

where, R is a 3X3 rotaion matrix, t is a 3X1 tranlation vector, and T[R|t] is a 4X4 homogeneous tranformation matrix.

Case 1: Known data association. where each point in source point cloud set p_i coressponds to q_j point in the target point cloud set with same index or to any known index. then, eq. (2.1) can be solved by finding the center of mass and singular value decomposition as follows.

center of mass for the source point cloud set and target point cloud set is

$$\begin{aligned}
\mu_p &= \frac{1}{\|C\|} \sum_{(i,j)\in C} p_i \\
\mu_q &= \frac{1}{\|C\|} \sum_{(i,j)\in C} q_i
\end{aligned} \tag{2.2}$$

By subtracting the center of mass from every point in the source and target point cloud, we get

$$\begin{aligned}
Q' &= \{q_i - \mu_q\} = \{q'_i\} \\
P' &= \{p_j - \mu_p\} = \{p'_j\}
\end{aligned} \tag{2.3}$$

minimizing eq. (2.1) is equivalent to minimizing,

$$\mathtt{E'(R)} = \sum_{(i,j)\in C} \|[q'_1, q'_2, ..., q'_n] - R[p'_1, p'_2, ..., p'_m]\|_F^2 \tag{2.4}$$

and is called orthogonal procrustes problem and can be solved by constructing cross-covariance matrix of 2 point cloud sets and SVD [16]. The cross-covariance matrix of 2 point cloud sets is,

$$W = \sum_{(i,j)\in C} \{q_i - \mu_q\}\{p_i - \mu_p\}^T$$
$$W = \sum_{(i,j)\in C} q_i' p_j'^T$$

(2.5)

Use the SVD to decompose the cross-covariance matrix hence find the transformation between the 2 point clouds.

$$W = UDV^T \text{ then,}$$
$$R = UV^T$$
$$t = \mu_q - R\mu_p$$

(2.6)

In conclusion, a point cloud matching algorithm estimates the 3X3 rotation matrix R and 3X1 traslation vector t.

$$(T[R|t], MSE) = PointCloudRegistration(P, Q)$$

where, T[R|t] is the 4X4 homogeneous transformation between source and target point cloud and MSE is the mean square error of matching as in eq. (2.1).

Case 2: Unnown data association. when the correspondece between source & target point cloud set is unknown, we resort to iterative closest point algorithm. Where for each point in the source point cloud set $P = \{p_1, p_2, ..., p_m\}$ coressponding closest point in the target point cloud $Q = \{q_1, q_2, ..., q_n\}$ is calculated before proceeding to the point cloud matching.

The Eucledian distance $d(\vec{p_1}, \vec{p_2})$ between two points $\vec{p_1} = (x_1, y_1, z_1)$ and $\vec{p_2} = (x_2, y_2, z_2)$ is

$$d(\vec{p_1}, \vec{p_2}) = \|\vec{p_1} - \vec{p_2}\| = \sqrt{(x_2 - x_1)^2 + (y_2 - y_1)^2 + (z_2 - z_1)^2}$$

The distance between a point p in the source point cloud set and the target point cloud set $Q = \{q_1, q_2, ..., q_n\}$, $d(\vec{p}, Q)$ is

$$d(\vec{p}, Q) = \min_{i \in Q} d(\vec{p}, \vec{q_i})$$

(2.7)

$$d(\vec{p}, Q) = \min_{i \in Q} \|\vec{p} - \vec{q_i}\|$$

The point in target point cloud $q* \in Q$ that yields a minimum distance is the closest point. The unknown data association is solved when closest point computation is performed for each point in the source point cloud set $P = \{p_1, p_2, ..., p_m\}$.

$$C = ComputeClosestPoint(P, Q) \tag{2.8}$$

where $C = \{(i, j)\}$ is the computed correspondence set for each point in the source point cloud. Having computed the corresponce set, one can proceed with point cloud registration. Each point the source point cloud is updated via $P_{k+1} = T[R|t]P_k$

$$P_{k+1} = ApplyRegistration(T[R|t], P_k) \tag{2.9}$$

where, P_{k+1} are the points after applying the registration (homogeneous represetation is used here to enable matrix multiplication).

2.1.1 Iterative closest point algorithm

1. Given $P = \{p_1, p_2, ..., p_m\}$ be the source point cloud set that needs to be aligned with the target point cloud set $Q = \{q_1, q_2, ..., q_n\}$ with unknown data association.

2. Initialize the iteration $P_0 = P$, $T[R|t] = $ 4X4 identity [], $k = 0$

   a) $C_k = ComputeClosestPoint(P_k, Q)$

   b) $(T[R|t]_k, MSE_k) = PointCloudRegistration(P_0, C_k)$

   c) $P_{k+1} = ApplyRegistration(T[R|t]_k, P_0)$

   d) Terminate the iteration when

      i. change in the mean square error is less than a predefined threshold $\tau > 0$ i.e. $MSE_k - MSE_{k+1} < \tau$.

      ii. or when iteration exceeds the predefined number.

2.2 Simultaneous Localization and Mapping

2.2.1 Map

A map of the environment is a collection of objects in the environment and their locations. Formally, a map m is a list of objects in the environment along with their properties [17]

$$m = \{m_1, m_2, ...m_N\}$$

where, N is the total number of objects in the environment and m_n where $1 \leq n \leq N$ represents the poperty of the object n. Maps are usually either feature-based or location-based. In feature based maps, m_n is a tuple of the feature property and feature (2D/3D) location. On the location-based maps, its only the (2D/3D) location.

2.2.2 Localization

In simple words, localization is the pose estimation problem. It is the process of determining the pose of a robot with respect to the given map of the enviornement using wide vareity of sensor data i.e perception sensors and wheel odometry etc. Localization is also the problem of establishing the correspondence between coordinate system based on which the map is defined (often, global coordinate system) and the robot's local coordinate system. This correspondence enables the robot to express the objects in the map in it's local coordinate system to be able to successfully navigate through the environment. Unfortunately, sensor measurements are noisy therefore pose has to be inferred from the noisy data which makes localization a difficult problem to solve. There are many probablistic approaches to solve localization problems, the reader is encouraged to refer [17] for more details.

2.2.3 SLAM

Simultaneous localization and mapping (SLAM) is a special case where the robot neither have the pre-build map of the environment nor does it know its pose with respect to the environment. Robot however has wide vareity of sensors onboard to percieve its environment along with the capability to move with in the environment. Robot's task is to build the map of the environment and simultaneously localize itself with this map. Due to the fact that measurements are prone to noise, SLAM problems are modelled probabalistically.

Probabilistic formulation of SLAM. The robot moves with in an unknown environment along a trajectory. Robot poses along the trajectory are described by the random variables $x_{1:t} = \{x_1, ..., x_t\}$

SLAM can be broadly classified in to 2 types, online-SLAM and full-SLAM.

Online-SLAM. Estimating the current pose and the map.

$$p(x_t, m | z_{1:t}, u_{1:t})$$

where x_t is the pose at current time t, m is map, $z_{1:t}$ and $u_{1:t}$ are measurement and control inputs untill the current time t respectively. Online-SLAM is essentially a online state estimation problem where state is the current robot pose and the map. The pose and the map is estimated and refined as and when the new measurements are avaiable. Online-SLAM problem is is modelled and solved using filtering techninques such as Kalman and information filters [18] [19] and partical filters [20].

Full-SLAM. Estimating the entire robot trajectory and the map instead of just momentary pose.

$$p(x_{1:t}, m | z_{1:t}, u_{1:t})$$

Full-SLAM estimates $x_{1:t}$ the entire trajectory of the robot and simulataneously mapping the environment by incororating full set of measurements and control inputs

$z_{1:t}$ and $u_{1:t}$. Smoothing techniques like [21] [22] are employed to solve the full-SLAM problems. The modern and intuitive approach for solving full-SLAM problem is to use graph-based formulation. Due to the improvements in the areas of computation power and efficient linear algebra solvers, graph-based formulations have undergone a renaissance since in inception [21].

2.3 Camera fundamenals

A gentle introduction to the pinhole camera model, projection matrix, calibration (internal and external), the underlying mathematics.
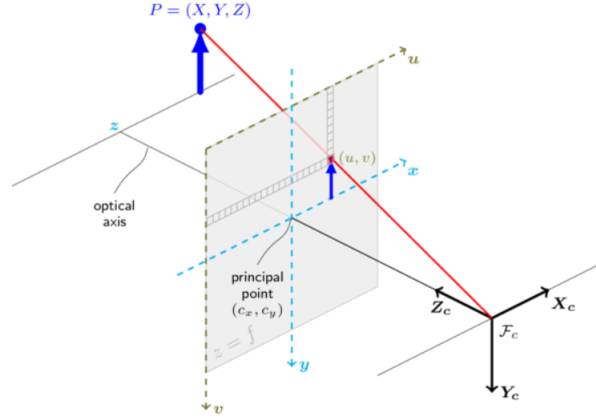

Fig. 2.1: Pinhole camera geometry. $\boldsymbol{F_c}$ *is the camera center,* (C_x, C_y) *is the principal point,* $\boldsymbol{P}$ $(X, Y, Z)^T$ *is world point,* $\boldsymbol{P_c}$ $(X_c, Y_c, Z_c)^T$ *is world point measured in camera coordinate system.[23]*

A simplified perspective projection is shown in fig. 2.1. A world point $(X_c, Y_c, Z_c)^T$ is mapped to $(f\frac{X_c}{Z_c}, f\frac{Y_c}{Z_c}, f)^T$ on the image plane placed at a focal length distance f from the camera center (F_c). Two key facts can be derived from the above projection equation that farther the object is (larger the Z_c) from the camera, smaller the size in image plane (shrinking operation) and these shrunk points are magnified by the focal length f to be placed on the image plane. World points are first shrunk $(x, y)^T = (\frac{X_c}{Z_c}, \frac{Y_c}{Z_c})^T$ and then magnified $(f\frac{X_c}{Z_c}, f\frac{Y_c}{Z_c}, f)^T$.

Often, the world points are represented in homogeneous coordinates due to several advantages, being able to express infinite quantities is one of them. The linear mapping between world and image points is evident in the homogeneous representation as shown below.

$$Z_c \begin{bmatrix} x \\ y \\ 1 \end{bmatrix} = \begin{bmatrix} f & 0 & 0 & 0 \\ 0 & f & 0 & 0 \\ 0 & 0 & 1 & 0 \end{bmatrix} \begin{bmatrix} X_c \\ Y_c \\ Z_c \\ 1 \end{bmatrix} \tag{2.10}$$

The linear mapping can be expressed in a compact form $\boldsymbol{x} = \mathtt{P}\boldsymbol{X_c}$ where $\boldsymbol{x}$ is a vector of image points, $\boldsymbol{X}$ is a vector of world points and P is a 3x4 homogeneous matrix called

camera projection matrix. In general, the origin of the image plane may not coincide with the principal point, therefore it is necessary to map the projected points to pixels before using the image for further use as show in fig. 2.2.
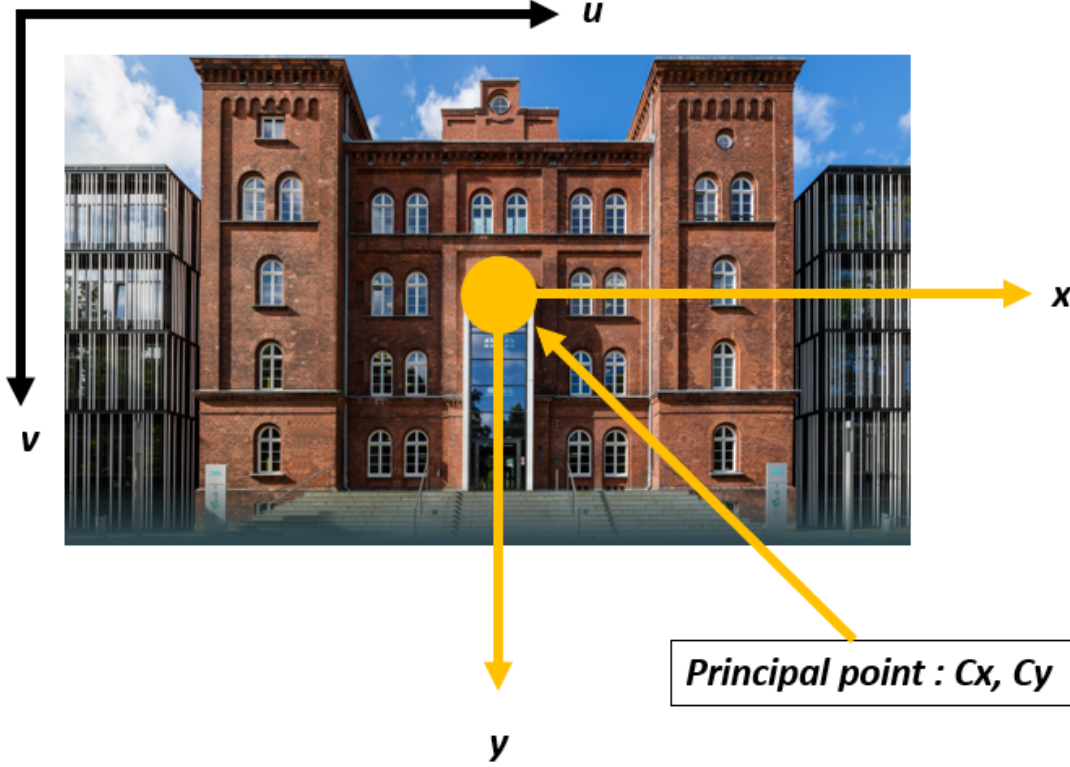

Fig. 2.2: Pixel coordinates (u, v) and the camera coordinates (x, y).

The equation 2.11 depicts mapping image to pixel coordinates. wehere (S_x) is size of pixel width and (S_y) is size of pixel height.

$$(u - C_x) = \frac{x}{S_x}$$
$$(v - C_y) = \frac{y}{S_y} \tag{2.11}$$

Therefore a 3D world point $(X_c, Y_c, Z_C)^T$ is mapped to $(f\frac{X}{Z} + C_x, f\frac{Y}{Z} + C_y, f)^T$ to the pixel coordinates (u, v, z) and can be expressed as a matrix multiplication. Where α_x is $(\frac{f}{S_x})$, α_y is $(\frac{f}{S_y})$ and S' is slant factor, when the image plane is not normal to the optical axis.

$$\begin{bmatrix} u \\ v \\ 1 \end{bmatrix} = \begin{bmatrix} \frac{1}{S_x} & S' & C_x \\ 0 & \frac{1}{S_y} & C_y \\ 0 & 0 & 1 \end{bmatrix} \begin{bmatrix} x \\ y \\ z \end{bmatrix} \tag{2.12}$$

$$Z_c \begin{bmatrix} u \\ v \\ 1 \end{bmatrix} = \begin{bmatrix} \alpha_x & S & C_x \\ 0 & \alpha_y & C_y \\ 0 & 0 & 1 \end{bmatrix} \begin{bmatrix} 1 & 0 & 0 & 0 \\ 0 & 1 & 0 & 0 \\ 0 & 0 & 1 & 0 \end{bmatrix} \begin{bmatrix} X_c \\ Y_c \\ Z_c \\ 1 \end{bmatrix} \tag{2.13}$$

$$Z_c \begin{bmatrix} u \\ v \\ 1 \end{bmatrix} = \begin{bmatrix} K_{3\times3} \end{bmatrix} \begin{bmatrix} I_{3\times3}|0 \end{bmatrix} \begin{bmatrix} X_c \\ Y_c \\ Z_c \\ 1 \end{bmatrix} \tag{2.14}$$

In summary, the equation 2.10 maps the world point measured in camera coordinates to image coordinates while equation 2.12 converts these image coordinates to pixel coordinates. Overall mapping from camera coordinates to the pixel coordinates is depicted in the equation 2.13. K in equation 2.14 is known as the camera intrinsic matrix and depends only on the internals of the camera. In general, a 3D world point $(X, Y, Z)^T$ may not be known in the camera coordinate system however it can be mapped using 4×4 homogeneous transformation matrix. equation 2.15 is a mapping from a 3D world point to pixel coordinates. The 4×4 homogeneous transformation matrix is known as an extrinsic matrix and describes the position and orientation of the 3D world point in the camera coordinate system.

$$Z_c \begin{bmatrix} u \\ v \\ 1 \end{bmatrix} = \begin{bmatrix} \alpha_x & S & C_x \\ 0 & \alpha_y & C_y \\ 0 & 0 & 1 \end{bmatrix} \begin{bmatrix} r_{11} & r_{12} & r_{13} & t_x \\ r_{21} & r_{22} & r_{23} & t_y \\ r_{31} & r_{32} & r_{33} & t_z \\ 0 & 0 & 0 & 1 \end{bmatrix} \begin{bmatrix} X \\ Y \\ Z \\ 1 \end{bmatrix} \tag{2.15}$$

The equation 2.15 can be compactly written by combining both intrinsic and extrinsic matrix known as the projection matrix P_{3X4}. Where P = K[R|t], and λ is a arbitrary scaling factor for which equation 2.16 is satisfied.

$$\lambda \begin{bmatrix} u \\ v \\ 1 \end{bmatrix} = \begin{bmatrix} p_{11} & p_{12} & p_{13} & p_{14} \\ p_{21} & r_{22} & r_{23} & p_{24} \\ p_{31} & p_{32} & p_{33} & p_{34} \end{bmatrix} \begin{bmatrix} X \\ Y \\ Z \\ 1 \end{bmatrix} \tag{2.16}$$

We extract the camera center from the projection matrix as the camera center C = $-R^{-1}t$ or in other words, $t = -RC$. Therefore the projection matrix can be written as,

$$\begin{aligned} \mathtt{P} &= \mathtt{K}\left[\mathtt{R} \mid \boldsymbol{t}\right] \\ &= \mathtt{KR}\left[\mathtt{I} \mid -\boldsymbol{C}\right] \\ &= \mathtt{M}\left[\mathtt{I} \mid \mathtt{M}^{-1} p_4\right] \end{aligned} \tag{2.17}$$

where M = KR, K is a 3x3 upper triangular camera matrix, R is a 3x3 rotation matrix and p_4 is the last column of the projection matrix.

2.4 Camera calibration

Often in practice, estimating intrinsic and extrinsic parameters are important and there are many ways to do so. Two approaches will be presented here, one using projection matrix from equation 2.16 (2D/3D correspondence) and using homography (2D/2D correspondence).
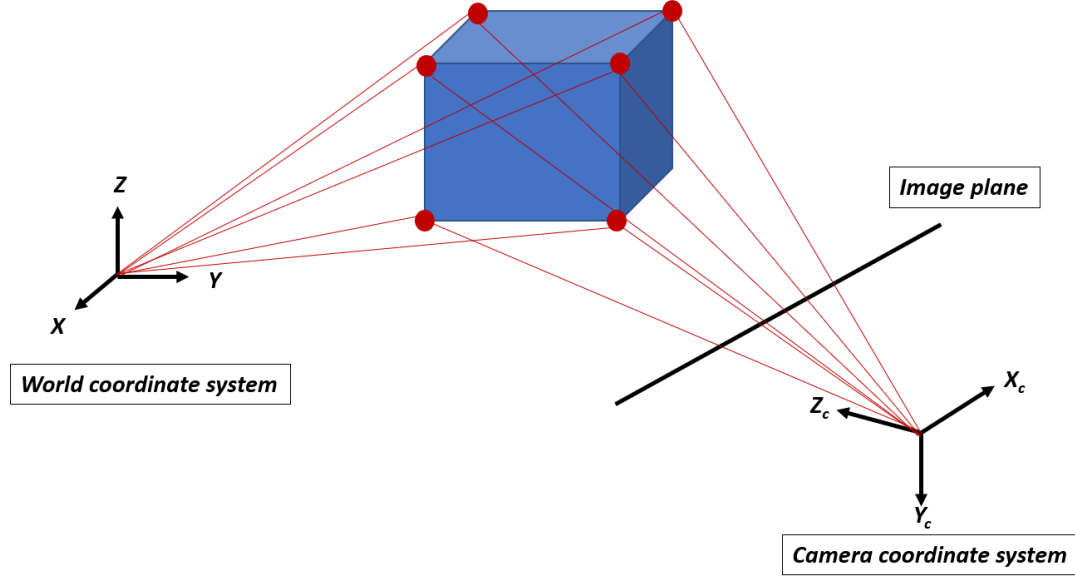
Fig. 2.3: Mapping 3D world points on to a 2D image plane.

2.4.1 2D/3D correspondence

The fig. 2.4 depicts a 2D image of a 3D object with known 6 unique points. Recall the equation 2.16 projection matrix P maps the world point to pixel coordinates and the equation is valid for arbitrary scaling factor λ. First, the projection matrix P will be estimated using a given set of 3D world points and 2D image points and then it will be decomposed to intrinsic and extrinsic matrices as P = K[R|t]. The first step in estimating projection matrix is to convert the equation 2.16 into least square problem of type II (see appendix) Ap = 0 subjected to $\|p\| = 1$ and solve for vector $\boldsymbol{p}$ which is reshaped version of non-trivial elements of the projection matrix P.

Given a set of N corresponding 2D/3D points (u_i, X_i), a projection matrix P is needed such that

$$\lambda u_i = PX_i \;, where\; i = 1......N$$

since the scaling factor λ is unknown and has to be estimated while estimating P. we will make use of DLT (direct linear transformation) to convert the above equation to the form Ap = 0.

$$
\begin{bmatrix} \lambda u_i \\ \lambda v_i \\ \lambda \end{bmatrix} =
\begin{bmatrix} p_{11} & p_{12} & p_{13} & p_{14} \\ p_{21} & r_{22} & r_{23} & p_{24} \\ p_{31} & p_{32} & p_{33} & p_{34} \end{bmatrix}
\begin{bmatrix} X_i \\ Y_i \\ Z_i \\ 1 \end{bmatrix}
$$

extracting the bottom row, equation for λ and substituting λ in other 2 rows yileds

$$\lambda = p_{31}X_i + p_{32}Y_i + p_{33}Z_i + p_{34}$$

$$u_i\lambda = u_i(p_{31}X_i + p_{32}Y_i + p_{33}Z_i + p_{34}) = p_{11}X_i + p_{12}Y_i + p_{13}Z_i + p_{14}$$
$$v_i\lambda = v_i(p_{31}X_i + p_{32}Y_i + p_{33}Z_i + p_{34}) = p_{21}X_i + p_{22}Y_i + p_{23}Z_i + p_{24}$$

Rearrangement of the above equations leads to a linear system of equations with non-trivial elements of the projection matrix being reshaped into a vector $\boldsymbol{p}$.

$$\begin{bmatrix} X_i & Y_i & Z_i & 1 & 0 & 0 & 0 & 0 & -u_iX_i & -u_iY_i & -u_iZ_i & -u_i \\ 0 & 0 & 0 & 0 & X_i & Y_i & Z_i & 1 & -v_iX_i & -v_iY_i & -v_iZ_i & -v_i \end{bmatrix} \mathbf{p} = \mathbf{0} \qquad (2.18)$$

$$with \ \mathbf{p} = \left(p_{11}, p_{12}.........p_{33}, p_{34}\right)^T \in \mathcal{R}^{12}$$

A projection matrix has 12 non-trivial elements thus 11 degrees of freedom (ignoring scaling) therefore it is necessary to have 11 equations to solve for P. Each pair of 2D/3D point correspondences leads to 2 equations thus a minimum of 6 2D/3D point correspondences are required. Stacking these 6 equations along rows leads to a linear system of equations Ap=0 as shown in eq. (2.19).

$$\begin{bmatrix} X_1 & Y_1 & Z_1 & 1 & 0 & 0 & 0 & 0 & -u_1X_1 & -u_1Y_1 & -u_1Z_1 & -u_1 \\ 0 & 0 & 0 & 0 & X_1 & Y_1 & Z_1 & 1 & -v_1X_1 & -v_1Y_1 & -v_1Z_1 & -v_1 \\ \vdots & \vdots & \vdots & \vdots & \vdots & \vdots & \vdots & \vdots & \vdots & \vdots & \vdots & \vdots \\ X_6 & Y_6 & Z_6 & 1 & 0 & 0 & 0 & 0 & -u_6X_6 & -u_6Y_6 & -u_6Z_6 & -u_6 \\ 0 & 0 & 0 & 0 & X_6 & Y_6 & Z_6 & 1 & -v_6X_i & -v_6Y_6 & -v_6Z_6 & -v_6 \end{bmatrix} \mathbf{p} = \mathbf{0} \qquad (2.19)$$

Exact solution. With a minimum of 6 correspondences, the solution to 2.19 will be exact which means 3D world points will be exactly gets projected to their measured image points correspondingly. The exact solution p, to $Ap = 0$ is the right nullspace of matrix A.

Over-determined solution. Practical measurements will be noisy due to various reasons and therefore we may require more than 6 2D/3D correspondences. In this case, the solution to $Ap = 0$ will be obtained by minimizing the algebraic or geometric error of projection, subjected to some valid constraints.

Minimizing algebraic error. In this case the approach is,

$$\min \quad \|Ap\| \quad \text{s.t.} \quad \|p\| = 1 \qquad (2.20)$$

The solution to eq. (2.20) is obtained from unit singular value of A corresponding to the smallest singular value (the least square problem of type II, see appendix).

Minimizing geometric error. First let us define what is geometric error. Let us recall eq. (2.16), $u_i = PX_i$, suppose we know 3D world points X_i far more accurately than the measured image points then the geometric error in the image is

$$\sum_{i=1}^{n} d(u_i, \hat{u}_i)^2$$

where u_i is measured point in the image and $\hat{u}_i$ is P X_i which is the exact projection of X_i on to the image under P. If the measurement errors are Gaussian then the solution to

$$\min_{P} \sum_{i=1}^{n} d(u_i, PX_i)^2 \qquad (2.21)$$

is the maximum likelihood of P as per [24]. Minimizing geometric error requires non-linear iterative methods such as Levenberg-Marquardt (LM) algorithms. Local minima can be found via LM, in order to find the global minima, the initial starting point can be linear solution obtained from eq. (2.20).

Having estimated projection matrix task at the hand is to decompose $P = K[R \mid t] = M[I \mid M^{-1} p_4]$ where $M = KR$. Decomposing M to K and R can be achieved using RQ decomposition with the constraint that diagonal entries of the K matrix has to be positive.
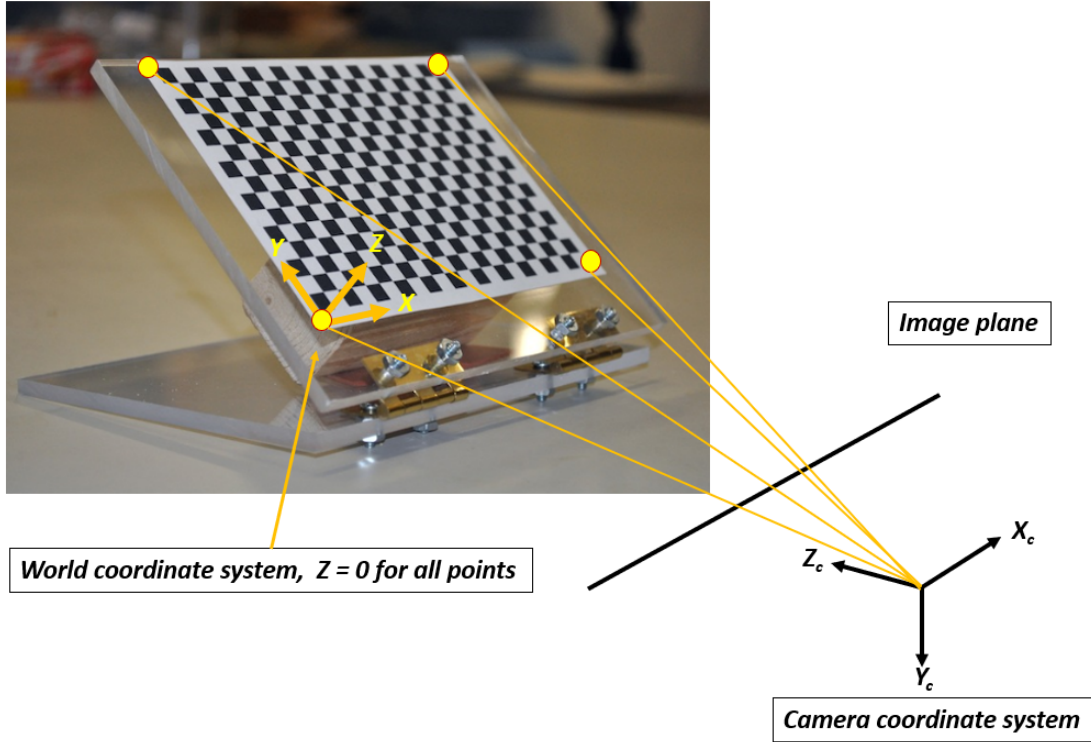
2.4.2 2D/2D correspondence

Fig. 2.4: Mapping 2D planar world points (Z = 0) on to a 2D image plane.

The disadvantage of 2D/3D correspondence way of estimating the projection matrix is that complete knowledge of the 3D location has to be known and it has to be precise as well. There is a flexible and computationally easy method to estimate the projection matrix thereby intrinsic and extrinsic camera parameters, developed by Zhang [25] using a 2D planar object in 3D space as shown in fig. 2.4 along with its 2D image. Let us recall the equation 2.15

$$Z_c \begin{bmatrix} u \\ v \\ 1 \end{bmatrix} = \begin{bmatrix} \alpha_x & S & C_x \\ 0 & \alpha_y & C_y \\ 0 & 0 & 1 \end{bmatrix} \begin{bmatrix} r_{11} & r_{12} & r_{13} & t_x \\ r_{21} & r_{22} & r_{23} & t_y \\ r_{31} & r_{32} & r_{33} & t_z \\ 0 & 0 & 0 & 1 \end{bmatrix} \begin{bmatrix} X \\ Y \\ Z \\ 1 \end{bmatrix}$$

Using 2D planar object we eliminate Z coordinate thereby eliminating 3rd column of the extrinsic matrix.

$$Z_c \begin{bmatrix} u \\ v \\ 1 \end{bmatrix} = \begin{bmatrix} \alpha_x & S & C_x \\ 0 & \alpha_y & C_y \\ 0 & 0 & 1 \end{bmatrix} \begin{bmatrix} r_{11} & r_{12} & r_{13} & t_x \\ r_{21} & r_{22} & r_{23} & t_y \\ r_{31} & r_{32} & r_{33} & t_z \\ 0 & 0 & 0 & 1 \end{bmatrix} \begin{bmatrix} X \\ Y \\ 0 \\ 1 \end{bmatrix}$$

$$Z_c \begin{bmatrix} u \\ v \\ 1 \end{bmatrix} = \begin{bmatrix} \alpha_x & S & C_x \\ 0 & \alpha_y & C_y \\ 0 & 0 & 1 \end{bmatrix} \begin{bmatrix} r_{11} & r_{12} & t_x \\ r_{21} & r_{22} & t_y \\ r_{31} & r_{32} & t_z \\ 0 & 0 & 1 \end{bmatrix} \begin{bmatrix} X \\ Y \\ 1 \end{bmatrix} \tag{2.22}$$

As in the case of 2D/3D problem setup, The equation 2.22 can be compactly written by combining both intrinsic and extrinsic matrices known an Homography matrix $H_{3\times3}$. And λ is a arbitrary scaling factor for which equation 2.23 is satisfied. In other words, A projection matrix $P_{3\times4}$ in planar case reduces to homography matrix $H_{3\times3}$.

$$\lambda \begin{bmatrix} u \\ v \\ 1 \end{bmatrix} = \begin{bmatrix} h_{11} & h_{12} & h_{13} \\ h_{21} & h_{22} & h_{23} \\ h_{31} & h_{32} & h_{33} \end{bmatrix} \begin{bmatrix} X \\ Y \\ 1 \end{bmatrix} \tag{2.23}$$

As in the case of 2D/3D problem, the homography matrix H will be estimated using a given set of 2D planar world points and 2D image points and then it will be decomposed to intrinsic and extrinsic matrices.

Given a set of N corresponding 2D/2D points (u_i, X_i), a homography matrix H is needed such that

$$\lambda u_i = H X_i \ , where \ i = 1......N$$

Problem set up in 2D/2D case is very similar to 2D/3D problem except that the homography matrix has 9 non-trivial elements thus 8 degrees of freedom (ignoring scaling) therefore 8 independent equations are necessary to estimate H, hence 4 2D/2D point correspondences are required. At this point, the same estimating procedure used previously can be employed.

Exact solution. With a minimum of 4 correspondences, the solution to $Ah = 0$ will be exact which means 2D world points will be exactly gets projected to their measured image points correspondingly. The exact solution h, to $Ah = 0$ is the right nullspace of matrix A.

Over-determined solution. In this case solution to $Ah = 0$ will be obtained by minimizing the algebraic or geometric error of projection, subjected to some valid constraints.

Minimizing algebraic error. In this case the approach is,

$$\min \quad ||Ah|| \quad \text{s.t.} \quad ||h|| = 1 \tag{2.24}$$

The solution to eq. (2.24) is obtained from unit singular value of A corresponding to the smallest singular value (the least square problem of type II, see appendix).

Minimizing geometric error The geometric error in the image in 2D/2D case is

$$\sum_{i=1}^{n} d(u_i, \hat{u}_i)^2$$

where u_i is measured point in image and $\hat{u}_i$ is H X_i which is the exact projrction of X_i on to the image under H. If the measurement errors are Gaussian then the solution to

$$\min_{P} \sum_{i=1}^{n} d(u_i, HX_i)^2 \tag{2.25}$$

is the maximum likelihood of H. Minimizing geometric error requires non-linear iterative methods such as Levenberg-Marquardt (LM) algorithms. Local minima can be found via LM, in order to find the global minima, initial starting point can be linear soution obtained from 2.20.

The disadvantage of 2D/2D homography is that with a single homography, not all the parameters of a projection matrix can be determined as Z coordinate of the world point is eliminated.

$$\mathbf{H} = \begin{bmatrix} \mathbf{p}_1 & \mathbf{p}_2 & \mathbf{p}_4 \end{bmatrix}$$

The decomposition of H to obtain extrinsic and intrinsic matrices is not possible, therefore, follows a different approach. We will first see how to get the intrinsic matrix K and as soon we have K, obtaining extrinsic is trivial.

Intrinsics Recall that $H = K \begin{bmatrix} \mathbf{r}_1 & \mathbf{r}_2 & \mathbf{t} \end{bmatrix} = [\mathbf{p}_1 \, \mathbf{p}_2 \, \mathbf{p}_3]$ and the fact that R is a rotational matrix and can be expressed as,

$$\mathbf{r}_1^\intercal \mathbf{r}_2 = 0$$
$$\mathbf{r}_1^\intercal \mathbf{r}_1 = \mathbf{r}_2^\intercal \mathbf{r}_2 = 1$$

rewriting with K gives,

$$\mathbf{p}_1^T K^{-T} K^{-1} \mathbf{p}_2 = 0$$
$$\mathbf{p}_1^T K^{-T} K^{-1} \mathbf{p}_1 = \mathbf{p}_2^T K^{-T} K^{-1} \mathbf{p}_2 = 1$$

defining $\omega = K^{-T} K^{-1}$ as a symmetric matrix, above equations can be written as,

$$\omega = \begin{bmatrix} \omega_{11} & \omega_{12} & \omega_{13} \\ \omega_{12} & \omega_{22} & \omega_{23} \\ \omega_{13} & \omega_{23} & \omega_{33} \end{bmatrix}$$

$$\mathbf{p}_1^T \omega \mathbf{p}_2 = 0$$
$$\mathbf{p}_1^T \omega \mathbf{p}_1 - \mathbf{p}_2^T \omega \mathbf{p}_2 = 0 \tag{2.26}$$

$\mathbf{p}_1$ and $\mathbf{p}_2$ are known from homography matrix and $\boldsymbol{\omega}$ has to be calculated. $\boldsymbol{\omega}$ can be estimated with techniques that we employed earlier with DLT and SVD by defining $\mathbf{b} = (\omega_{11} \; \omega_{12} \; \omega_{13} \; \omega_{22} \; \omega_{23} \; \omega_{33})^T$ and solving $\mathbf{Ab} = 0$. Each homography provides 2 independent rows therfore 3 such homographies are required to estimate $\boldsymbol{\omega}$. Once the $\boldsymbol{\omega}$

is computed it can be decomposed in to $K^{-T}K^{-1}$ using Cholesky decomposition.

Extrinsics. Computing extrinsics post intrinsics is very straight forward as given by [25] we will first calculate rotation matrix followed by translation vector. $H = K \left[\mathbf{r}_1 \ \mathbf{r}_2 \ \mathbf{t}\right]$ having known K we can rearrange as $K^{-1} \ H = H^{'} = [\mathbf{h}_1^{'} \ \mathbf{h}_2^{'} \ \mathbf{h}_3^{'}]$ which is theoritically equal to $[\mathbf{r}_1 \ \mathbf{r}_2 \ \mathbf{t}]$. Since the rotational matrix is a orthogonal matrix, third column is othogonal to first 2 and therefore can be calculated by vector cross product $[\mathbf{h}_1^{'} \times \mathbf{h}_2^{'}]$ hence, the complete rotational matrix is $Q = [\mathbf{h}_1^{'} \ \mathbf{h}_2^{'} \ \mathbf{h}_1^{'} \times \ \mathbf{h}_2^{'}]$ again which is theoritically equal to $R = [\mathbf{r}_1 \ \mathbf{r}_2 \ \mathbf{r}_1 \ \times \ \mathbf{r}_2 \ ]$ which may not be true due to the noisy data. Therefore, it necessary to find a best 3x3 rotation matrix R from a given 3x3 matrix Q, here "best" in the sense of smallest Frobenius norm of the difference $[R - Q]$ (see appendix). If the SVD of given matrix is $Q = UDV^T$, then the best rotation matrix is given by UV^T. The translation vector can be calculated as $\mathbf{t} = \mathbf{h}_3^{'}$ but the vector $\mathbf{t}$ has to be normalised therefore $\mathbf{t} = \mathbf{h}_3^{'}/\|\mathbf{h}_1^{'}\|$.

2.4.3 Lens distortions

A world point is mapped to image plane as $(x, y, z)^T = (f\frac{X_c}{Z_c}, f\frac{Y_c}{Z_c}, f)^T$ then image points are mapped to pixel coordinates as $(u, v, z)^T = (x + C_x, y + C_y, f)^T$ however, usually, there are radial and tangential distortions in the lens as depicted in fig. 2.5 therefore, image coordinates have to be corrected before mapping to pixel coordinates. The corrected image coordinates are

$$
\begin{aligned}
x^{'} &= x \times \frac{1 + k_1 r^2 + k_2 r^4 + k_3 r^6}{1 + k_4 r^2 + k_5 r^4 + k_6 r^6} + 2p_1 xy + p_2(r^2 + 2x^2) \\
y^{'} &= y \times \frac{1 + k_1 r^2 + k_2 r^4 + k_3 r^6}{1 + k_4 r^2 + k_5 r^4 + k_6 r^6} + p_1(r^2 + 2y^2) + 2p_2 xy
\end{aligned}
\tag{2.27}
$$

where $r^2 = (x^2 + y^2)$, $k_1.....k_6$ are the radial distortion coefficients and p_1, p_2 are the tangential distortion coefficients. It is these corrected image coordinates are mapped to pixel coordinates as $(u, v, z)^T = (x^{'} + C_x, y^{'} + C_y, f)^T$.

No distortion — Positive radial distortion (Barrel distortion) — Negative radial distortion (Pincushion distortion)
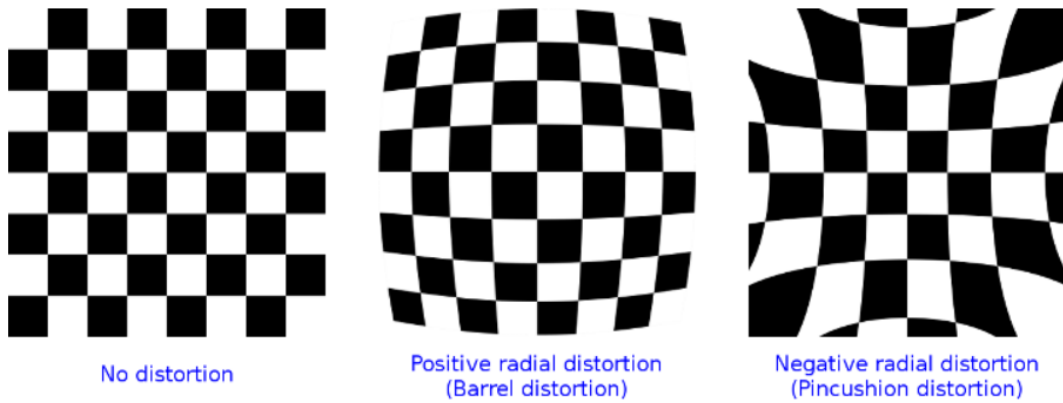
Fig. 2.5: Barrel distortion (*typically* $k_1 > 0$) and pincushion distortion (*typically* $k_1 < 0$) [23]

Camera calibration is the process of determining, intrinsic, extrinsic parameters along with distortion coefficients. The tab. 2.1 summarizes the calibration process discussed above.

Tab. 2.1: Calibration summary table

correspondences	Min. points	No.of images	[R | t]	K	world points
2D im./3D world	≥ 6	1	✓	✓	given
2D im./2D world	≥ 4	3	✓	✓	given
2D im./2D world	≥ 4	1	✓	given	given

2.5 Camera calibration and pose estimation

Camera calibration is carried out using open-source computer vision library OpenCV [23]. Camera calibration is based on 2D/2D point correspondences with the chessboard as a 2D planar object. The homography is calculated using square corners of a chessboard (world points) and its image points. OpenCV needs an arrays of world points and image points and the grid size of the chessboard (in our case its 5 rows, 8 columns). Therefore, 10 RGB images of the chessboard at different position and orientation was recorded and an array of world points (x,y) location of chessboard corners [(0,0), (40,0), (80,0)...] was fed to the algorithm. OpenCV automatically detects these chessboard corners from the images as shown in fig. 2.6 and refines them accordingly.
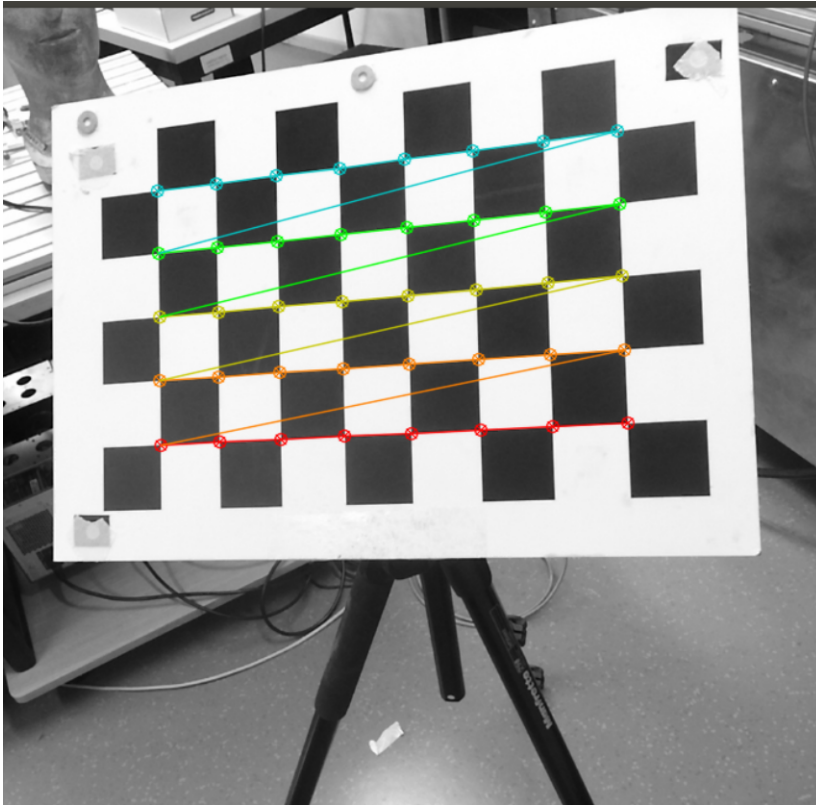

Fig. 2.6: Chessboard corners(image points) detection in OpenCV

```
cv2.calibrateCamera(object_points, image_points, ...)
output: rms, camera_matrix, dist_coeffs, rot_vecs, trans_vecs
```

The OpenCV function cv2.calibrateCamera takes in these world points (object points), image points and some more arguements then outputs geometric error of reprojection (rms), intrinsic parameters (camera_matrix) distortion coefficients (dist_coeffs) and extrinsic parameters ($rot\_vecs, trans\_vecs$).

Having completed the camera calibration we can now make use of the intrinsic parameters and the distortion coefficients as an input to the pose estimation algorithm provided by OpenCV.

```
cv2.solvePnP(object_points, image_points, intr_mat, dist_coeffs)
output: rot_vecs, trans_vecs
```

The OpenCV function cv2.solvePnP takes object points, image points, intrinsic matrix, and distortion coeffcients as the arguments and computes rotation and translation vectors. Rotation vector can be converted to 3×3 rotational matrix using cv2.Rodrigues function provided by openCV. By combining rotation matrix and translation vector we can form 4×4 homogenious matrix for further manipulation.

Bibliography

[1] en.wikipedia.org. (1999). "MS Windows NT kernel description," [Online]. Available: `https://en.wikipedia.org/wiki/Electroencephalography` (visited on 05/20/2020).

[2] S. Qian and Y. Sheng, "A single camera photogrammetry system for multi-angle fast localization of eeg electrodes," *Annals of biomedical engineering*, vol. 39, pp. 2844–56, Aug. 2011. DOI: `10.1007/s10439-011-0374-6`.

[3] C. Binnie, E Dekker, A Smit, and G Van der Linden, "Practical considerations in the positioning of eeg electrodes," *Electroencephalography and Clinical Neurophysiology*, vol. 53, no. 4, pp. 453–458, 1982.

[4] J. De Munck, P. Vijn, and H. Spekreijse, "A practical method for determining electrode positions on the head," *Electroencephalography and clinical Neurophysiology*, vol. 78, no. 1, pp. 85–87, 1991.

[5] D. Khosla, M. Don, and B. Kwong, "Spatial mislocalization of eeg electrodes–effects on accuracy of dipole estimation," *Clinical neurophysiology*, vol. 110, no. 2, pp. 261–271, 1999.

[6] J. Le, M. Lu, E. Pellouchoud, and A. Gevins, "A rapid method for determining standard 10/10 electrode positions for high resolution eeg studies," *Electroencephalography and clinical neurophysiology*, vol. 106, no. 6, pp. 554–558, 1998.

[7] S Steddin and K Bötzel, "A new device for scalp electrode localization with unrestrained head," *J. Neurol*, vol. 242, p. 65, 1995.

[8] L. Koessler, T. Cecchin, O. Caspary, A. Benhadid, H. Vespignani, and L. Maillard, "Eeg–mri co-registration and sensor labeling using a 3d laser scanner," *Annals of Biomedical Engineering*, vol. 39, no. 3, pp. 983–995, 2011.

[9] H. Bauer, C. Lamm, S. Holzreiter, I. Holländer, U. Leodolter, and M. Leodolter, "Measurement of 3d electrode coordinates by means of a 3d photogrammetric head digitizer," *NeuroImage*, vol. 11, no. 5, S461, 2000.

[10] G. S. Russell, K. J. Eriksen, P. Poolman, P. Luu, and D. M. Tucker, "Geodesic photogrammetry for localizing sensor positions in dense-array eeg," *Clinical Neurophysiology*, vol. 116, no. 5, pp. 1130–1140, 2005.

[11] L. Koessler, L. Maillard, A. Benhadid, J.-P. Vignal, M. Braun, and H. Vespignani, "Spatial localization of eeg electrodes," *Neurophysiologie Clinique/Clinical Neurophysiology*, vol. 37, no. 2, pp. 97–102, 2007.

[12] U. Baysal and G. Şengül, "Single camera photogrammetry system for eeg electrode identification and localization," *Annals of biomedical engineering*, vol. 38, no. 4, pp. 1539–1547, 2010.

[13] S. Chen, Y. He, H. Qiu, X. Yan, and M. Zhao, "Spatial localization of eeg electrodes in a tof+ ccd camera system," *Frontiers in neuroinformatics*, vol. 13, p. 21, 2019.

[14] P. J. Besl and N. D. McKay, "Method for registration of 3-d shapes," in *Sensor fusion IV: control paradigms and data structures*, International Society for Optics and Photonics, vol. 1611, 1992, pp. 586–606.

[15] G. Grisetti, R. Kümmerle, C. Stachniss, and W. Burgard, "A tutorial on graph-based slam," *IEEE Intelligent Transportation Systems Magazine*, vol. 2, no. 4, pp. 31–43, 2010.

[16] I. Söderkvist, "Using svd for some fitting problems," *University Lecture*, 2009.

[17] S. Thrun, W. Burgard, and D. Fox, *Probabilistic Robotics (Intelligent Robotics and Autonomous Agents)*. The MIT Press, 2005, ISBN: 0262201623.

[18] R. Smith, M. Self, and P. Cheeseman, "Estimating uncertain spatial relationships in robotics," in *Autonomous robot vehicles*, Springer, 1990, pp. 167–193.

[19] J. A. Castellanos, J. Montiel, J. Neira, and J. D. Tardós, "The spmap: A probabilistic framework for simultaneous localization and map building," *IEEE Transactions on robotics and Automation*, vol. 15, no. 5, pp. 948–952, 1999.

[20] M. Montemerlo, S. Thrun, D. Koller, B. Wegbreit, *et al.*, "Fastslam: A factored solution to the simultaneous localization and mapping problem," *Aaai/iaai*, vol. 593598, 2002.

[21] F. Lu and E. Milios, "Globally consistent range scan alignment for environment mapping," *Autonomous robots*, vol. 4, no. 4, pp. 333–349, 1997.

[22] F. Dellaert and M. Kaess, "Square root sam: Simultaneous localization and mapping via square root information smoothing," *The International Journal of Robotics Research*, vol. 25, no. 12, pp. 1181–1203, 2006.

[23] opencv.org. (1999). "MS Windows NT kernel description," [Online]. Available: https://docs.opencv.org/2.4/modules/calib3d/doc/camera_calibration_and_3d_reconstruction.html (visited on 05/20/2020).

[24] R. Hartley and A. Zisserman, *Multiple View Geometry in Computer Vision*, 2nd ed. New York, NY, USA: Cambridge University Press, 2003, ISBN: 0521540518.

[25] Z. Zhang, "A flexible new technique for camera calibration," *IEEE Transactions on Pattern Analysis and Machine Intelligence*, vol. 22, no. 11, pp. 1330–1334, 2000, ISSN: 0162-8828. DOI: 10.1109/34.888718.

Declaration

Hiermit versichere ich, dass ich meine Abschlussarbeit selbständig verfasst und keine anderen als die angegebenen Quellen und Hilfsmittel benutzt habe.

Datum: ....
(Unterschrift)